Recognition of an organism from fragments of its complete genome

V. V. Anh,[1,*] K. S. Lau,[2,†] and Z. G. Yu[1,3,‡]

[1]*Centre in Statistical Science and Industrial Mathematics, Queensland University of Technology, P. O. Box 2434,*
Brisbane Q4001, Australia
[2]*Department of Mathematics, Chinese University of Hong Kong, Shatin, Hong Kong*
[3]*Department of Mathematics, Xiangtan University, Hunan 411105, People's Republic of China*

This paper considers the problem of matching a fragment to an organism using its complete genome. Our method is based on the probability measure representation of a genome. We first demonstrate that these probability measures can be modeled as recurrent iterated function systems (RIFS) consisting of four contractive similarities. Our hypothesis is that the multifractal characteristics of the probability measure of a complete genome, as captured by the RIFS, is preserved in its reasonably long fragments. We compute the RIFS of fragments of various lengths and random starting points, and compare with that of the original sequence for recognition using the Euclidean distance. A demonstration on five randomly selected organisms supports the above hypothesis.

I. INTRODUCTION

The DNA sequences of complete genomes provide essential information for understanding gene functions and evolution. A large number of these DNA sequences is currently available in public databases, such as Genbank at ftp://ncbi.nlm.nih.gov/genbank/genomes/ or KEGG at http://www.genome.ad.jp/kegg/java/org_list.html. A great challenge of DNA analysis is to determine the intrinsic patterns contained in these sequences, which are formed by four basic nucleotides, namely, adenine (a), cytosine (c), guanine (g), and thymine (t).

Some significant results have been obtained for the long-range correlation in DNA sequences [1–16]. Li and Kaneko [1] found that the spectral density of a DNA sequence containing mostly introns shows $1/f^\beta$ behavior, which indicates the presence of long-range correlation when $0 < \beta < 1$. The correlation properties of coding and noncoding DNA sequences were first studied by Peng *et al.* [2] in their fractal landscape or DNA walk model. The DNA walk [2] was defined as that the walker steps "up" if a pyrimidine (c or t) occurs at position i along the DNA chain, while the walker steps "down" if a purine (a or g) occurs at position i. Peng *et al.* [2] discovered that there exists long-range correlation in noncoding DNA sequences while the coding sequences correspond to a regular random walk. By undertaking a more detailed analysis, Chatzidimitriou-Dreismann and Larhammar [5] concluded that both coding and noncoding sequences exhibit long-range correlation. A subsequent work by Prabhu and Claverie [6] also substantially corroborates these results. If one considers more details by distinguishing c from t in pyrimidine and a from g in purine (such as two- or three-dimensional DNA walk models [15] and maps given by Yu

and Chen [16]), then the presence of base correlation has been found even in the coding sequences. On the other hand, Buldyrev *et al.* [12] showed that long-range correlation appears mainly in noncoding DNA using all the DNA sequences available. Based on equal-symbol correlation, Voss [8] showed a power law behavior for the sequences studied, regardless of the proportion of intron contents. These studies add to the controversy about the possible presence of correlation in the entire DNA or only in the noncoding DNA. From a different angle, fractal analysis has proven useful in revealing complex patterns in natural objects. Berthelsen *et al.* [17] considered the global fractal dimensions of human DNA sequences treated as pseudorandom walks.

In the above studies, the authors only considered short or long DNA segments. Since the first complete genome of the free-living bacterium *Mycoplasma genitalium* was sequenced in 1995 [18], an ever-growing number of complete genomes has been deposited in the public databases. The availability of complete genomes induces the possibility to establish some global properties of these sequences. Vieira [19] carried out a low-frequency analysis of the complete DNA of 13 microbial genomes and showed that their fractal behavior does not always prevail, through the entire chain and the autocorrelation functions have a rich variety of behaviors including the presence of antipersistence. Yu and Wang [20] proposed a time series model of coding sequences in complete genomes. For more details on the number, size, and ordering of genes along the chromosome, one can refer to Part 5 of Lewin [21]. One may ignore the composition of the four kinds of bases in coding and noncoding segments and only consider the global structure of the complete genomes or long DNA sequences. Provata and Almirantis [22] proposed a fractal Cantor pattern of DNA. They mapped coding segments to filled regions and noncoding segments to empty regions of a random Cantor set and then calculated the fractal dimension of this set. They found that the coding/noncoding partition in DNA sequences of lower organisms is homogeneouslike, while in the higher eukaryotes the partition is fractal. This result does not seems to be refined enough to

---

*Email address: v.anh@qut.edu.au

†Email address: kslau@math.cuhk.edu.hk

‡Author to whom correspondence should be addressed. Email address: yuzg@hotmail.com or z.yu@qut.edu.au

distinguish bacteria because the computed fractal dimensions of bacteria [22] are the same. The classification and evolution relationship of bacteria is one of the most important problems in DNA research. Yu and Anh [23] proposed a time series model based on the global structure of the complete genome and considered three kinds of length sequences. After calculating the correlation dimensions and Hurst exponents, it was found that one can get more information from this model than that of the fractal Cantor pattern. Some results on the classification and evolution relationship of bacteria were found [23]. The correlation property of these length sequences has been discussed [24]. The multifractal analysis for these length sequences was done in Ref. [25].

Although statistical analysis performed directly on DNA sequences has yielded some success, there has been some indication that this method is not powerful enough to amplify the difference between a DNA sequence and a random sequence, as well as to distinguish DNA sequences, themselves in more detail [26]. One needs more powerful global and visual methods. For this purpose, Hao *et al.* [26] proposed a visualization method based on counting and coarse graining the frequency of appearance of substrings with a given length. They called it the *portrait* of an organism. They found that there exist some fractal patterns in the portraits, which are induced by avoiding and underrepresented strings. The fractal dimension of the limit set of portraits was also discussed [27,28]. There are other graphical methods of sequence patterns, such as the chaos game representation [29,30].

Yu *et al.* [31] introduced a representation of a DNA sequence by a probability measure of k strings derived from the sequence. This probability measure is, in fact, the histogram of the events formed by all the k strings in a dictionary ordering. It was found [31] that these probability measures display a distinct multifractal behavior characterized by their generalized Rényi dimensions (instead of a single fractal dimension as in the case of a self-similar process). Furthermore, the corresponding C_q curves (defined in Ref. [32]) of these generalized dimensions of all bacteria resemble classical phase transition at a critical point, while the "analogous" phase transitions (defined in Ref. [32]) of chromosomes of nonbacteria exhibit the shape of double-peaked specific heat function. These patterns led to a meaningful grouping of archaebacteria, eubacteria, and eukaryotes. Anh *et al.* [33] took a further step in providing a theory to characterize the multifractality of the probability measures of the complete genomes. In particular, the resulting parametric models fit extremely well the D_q curves of the generalized dimensions and the corresponding K_q curves of the above probability measures of the complete genomes.

A conclusion of the work reported by Yu *et al.* [31] and Anh *et al.* [33] is that the histogram of the k strings of the complete genome provides a good representation of the genome and that these probability measures are multifractal. This multifractality is, in most of the cases studied, characteristic of the DNA sequences, and hence can be used for their classification.

In this paper, we consider the problem of recognition of an organism based on fragments of their complete genomes.

The identification of the organisms in a culture commonly relies on their molecular identity markers such as the genes that code for ribosomal RNA. However, it is usual that most fragments lack the marker, "making the task of matching fragment to organism akin to reconstructing a document that has been shredded" (M. Leslie, "Tales of the sea," *New Scientist*, 27 January 2001). A well-known method to tackle the task is the random shotgun sequencing method that scans the sequences of all fragments looking for overlaps to be able to piece the fragments together. It is obvious that this technique is extremely time consuming and many crucial fragments may be missing.

This paper will provide a different method to approach this problem. Our starting point is the probability measure of the k strings and its multifractality. We model this multifractality using a recurrent iterated function system [34,35] consisting of four contractive similarities (to be described in Sec. IV). This branching number of 4 is a natural consequence of the four basic elements (a,c,g,t) of the DNA sequences. Each of these recurrent iterated function systems (RIFS) is specified by a matrix of incidence probabilities $\mathbf{P} = (p_{ij})$, $i,j = 1,\ldots,4$, with $p_{i1} + p_{i2} + p_{i3} + p_{i4} = 1$ for $i = 1,\ldots,4$. It is our hypothesis that, for reasonably long fragments, the multifractal characteristic of the measure of a complete genome as captured by the matrix $\mathbf{P}$ is preserved in the fragments. We thus represent each fragment by a vector $[(\frac{1}{4}(p_{11} + p_{21} + p_{31} + p_{41}), \quad \frac{1}{4}(p_{12} + p_{22} + p_{32} + p_{42}), \quad \frac{1}{4}(p_{13} + p_{23} + p_{33} + p_{43})]$ in $\mathbf{R}_+^3$. We will see that for fragments of lengths longer than 1/20 of the original sequence and with random starting points, these vectors are very close, using the Euclidean distance, to the vector of the complete sequence.

We will demonstrate the technique on five organisms, namely, *A. fulgidus, B. burgdorferi, C. trachomatis, E. coli,* and *M. genitalium.* As remarked by Yu *et al.* [31], substrings of length $k = 6$ are sufficient to represent DNA sequences. For each organism, we compute the histograms for the 6 strings of its complete genome and four cases of fragments of lengths 1/4, 1/8, 1/15, and 1/20 of the complete sequence. The starting position of each fragment is chosen randomly. The RIFS of the complete genome and each of the fragments are computed next. The numerical results are reported in Sec. V. Some conclusions will be drawn in Sec. VI.

II. MEASURE REPRESENTATION OF COMPLETE GENOMES

We first outline the method of Yu *et al.* [31] in deriving the measure representation of a DNA sequence. We call any string made up of k letters from the set $\{g,c,a,t\}$ a k string. For a given k there are a total of 4^k different k strings. In order to count the number of each kind of k strings in a given DNA sequence, 4^k counters are needed. We divide the interval $[0,1)$ into 4^k disjoint subintervals, and use each subinterval to represent a counter. Let $s = s_1,\ldots,s_k$, $s_i \in \{a,c,g,t\}, i = 1,\ldots,k$, be a substring with length k, we define
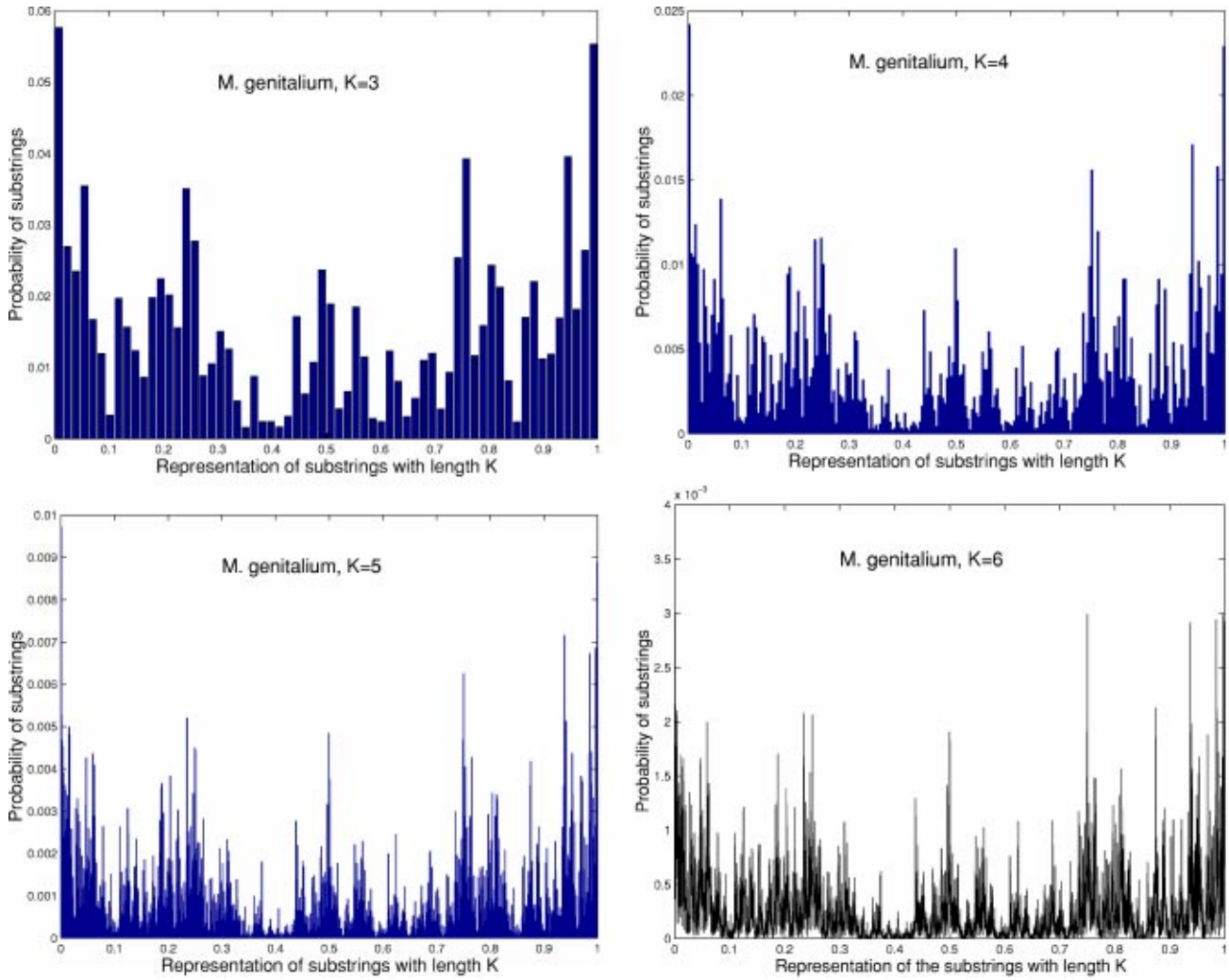
FIG. 1. Histograms of substrings with different lengths.

$$x_l(s) = \sum_{i=1}^{k} \frac{x_i}{4^i}, \tag{1}$$

where

$$x_i = \begin{cases} 0 & \text{if } s_i = a \\ 1 & \text{if } s_i = c \\ 2 & \text{if } s_i = g \\ 3 & \text{if } s_i = t \end{cases} \tag{2}$$

and

$$x_r(s) = x_l(s) + \frac{1}{4^k}. \tag{3}$$

We then use the subinterval $[x_l(s), x_r(s))$ to represent the substring s. Let $N(s)$ be the times of substring s appearing in the complete genome. If the number of bases in the complete genome is L, we define

$$F(s) = N(s)/(L - k + 1) \tag{4}$$

to be the frequency of substring s. It follows that $\Sigma_{\{s\}} F(s) = 1$. We can now view $F(s)$ as a function of x and define a measure μ_k on $[0,1)$ by

$$\mu_k(x) = Y_k(x) dx,$$

where

$$Y_k(x) = 4^k F_k(s), \quad x \in [x_l(s), x_r(s)). \tag{5}$$

We then have $\mu_k([0,1)) = 1$ and $\mu_k([x_l(s), x_r(s))) = F_k(s)$. We call $\mu_k(x)$ the *measure representation* of an organism. As an example, the measure representation of *M. genitalium* for $k = 3, \ldots, 6$ is given in Fig. 1. A fractal-like behavior is apparent in the measures.

Remark: The ordering of a, c, g, t in Eq. (2) follows the natural dictionary ordering of k strings in the one-dimensional space. A different ordering of a, c, g, t would change the nature of the correlations of the measure. But in our case, a different ordering of a, c, g, t in Eq. (2) gives the same multifractal spectrum (D_q curve, which will be defined in the following section) when the absolute value of q is relatively small (see Fig. 2 in Ref. [31]). Hence the multi-

fractal characteristics is independent of the ordering. In the comparison of different organisms using the measure representation, once the ordering of a,c,g,t in Eq. (2) is given, it is fixed for all organisms [31].

III. MULTIFRACTAL ANALYSIS

The most common algorithms of multifractal analysis are the so-called *fixed-size box-counting algorithms* [36]. In the one-dimensional case, for a given measure μ with support $E \subset \mathbf{R}$, we consider the *partition sum*

$$Z_\epsilon(q) = \sum_{\mu(B) \neq 0} [\mu(B)]^q, \tag{6}$$

$q \in \mathbf{R}$, where the sum runs over all different nonempty boxes B of a given side ϵ in a grid covering of the support E, that is,

$$B = [k\epsilon, (k+1)\epsilon]. \tag{7}$$

The exponent $\tau(q)$ is defined by

$$\tau(q) = \lim_{\epsilon \to 0} \frac{\ln Z_\epsilon(q)}{\ln \epsilon}, \tag{8}$$

and the generalized fractal dimensions of the measure are defined as

$$D_q = \tau(q)/(q-1) \quad \text{for} \quad q \neq 1, \tag{9}$$

and

$$D_q = \lim_{\epsilon \to 0} \frac{Z_{1,\epsilon}}{\ln \epsilon} \quad \text{for} \quad q = 1, \tag{10}$$

where $Z_{1,\epsilon} = \Sigma_{\mu(B) \neq 0} \mu(B) \ln \mu(B)$. The generalized fractal dimensions are estimated through a linear regression of

$$\frac{1}{q-1} \ln Z_\epsilon(q)$$

against $\ln \epsilon$ for $q \neq 1$, and similarly through a linear regression of $Z_{1,\epsilon}$ against $\ln \epsilon$ for $q = 1$. D_1 is called *information dimension* and D_2 is called *correlation dimension*. The D_q of the positive values of q give relevance to the regions where the measure is large, i.e., to the k strings with high probability. The D_q of the negative values of q deal with the structure and the properties of the most rarefied regions of the measure.

IV. IFS AND RIFS MODELS AND THE MOMENT METHOD FOR PARAMETER ESTIMATION

In this paper, we propose to model the measure defined in Sec. II for a complete genome by a recurrent IFS. As we work with measures on compact intervals, the theory of Sec. II is narrowed down to the one-dimensional case (i.e., $d = 1$). Consider a system of contractive maps $S = \{S_1, S_2, \ldots, S_N\}$. Let E_0 be a compact interval of $\mathbf{R}$,

$$E_{\sigma_1 \sigma_2 \cdots \sigma_n} = S_{\sigma_1} \circ S_{\sigma_2} \circ \cdots \circ S_{\sigma_n}(E_0) \text{ and}$$

$$E_n = \cup_{\sigma_1, \ldots, \sigma_n \in \{1,2,\ldots,N\}} E_{\sigma_1 \sigma_2 \cdots \sigma_n}.$$

Then $E = \cap_{n=1}^\infty E_n$ is the *attractor* of the IFS. Given a set of probabilities $p_i > 0$, $\Sigma_{i=1}^N p_i = 1$, we pick an $x_0 \in E$ and define iteratively the sequence

$$x_{n+1} = S_{\sigma_n}(x_n), \quad n = 0,1,2,\ldots, \tag{11}$$

where the indices σ_n are chosen randomly and independently from the set $\{1,2,\ldots,N\}$ with probabilities $P(\sigma_n = i) = p_i$. Then every orbit $\{x_n\}$ is dense in the attractor E [37,38]. For n large enough, we can view the orbit $\{x_0, x_1, \ldots, x_n\}$ as an approximation of E. This iterative process is called a *chaos game*.

Given a system of contractive maps $S = \{S_1, S_2, \ldots, S_N\}$ on a compact metric space E^*, we associate with these maps a matrix of probabilities $\mathbf{P} = (p_{ij})$ such that $\Sigma_j p_{ij} = \mathbf{1}$, $i = 1,2,\ldots,N$. Consider a random sequence generated by a chaos game,

$$x_{n+1} = S_{\sigma_n}(x_n), \quad n = 0,1,2,\ldots, \tag{12}$$

where x_0 is any starting point and σ_n is chosen with a probability that depends on the previous index σ_{n-1}:

$$P(\sigma_{n+1} = i) = p_{\sigma_n, i}. \tag{13}$$

The choice of the indices σ_n as prescribed by Eq. (13) presents a fundamental difference between this iterative process and that defined by Eq. (11) of the usual chaos game. Then $(E^*, S, \mathbf{P})$ is called a *recurrent* IFS. The flexibility of RIFS permits the construction of more general sets and measures which do not have to exhibit the strict self-similarity of IFS. This would offer a more suitable framework to model fractal-like objects and measures in nature.

Let μ be the invariant measure on the attractor E of an IFS or RIFS and χ_B the characteristic function for the Borel subset $B \subset E$, then from the ergodic theorem for IFS or RIFS [37],

$$\mu(B) = \lim_{n \to \infty} \left[\frac{1}{n+1} \sum_{k=0}^n \chi_b(x_k) \right]. \tag{14}$$

In other words, $\mu(B)$ is the relative visitation frequency of B during the chaos game. A histogram approximation of the invariant measure may then be obtained by counting the number of visits made to each pixel on the computer screen.

The coefficients in the contractive maps and the probabilities in the IFS or RIFS model are the parameters to be estimated for a given measure which we want to simulate. Vrscay [38] introduced a moment method to perform this task. If μ is the invariant measure and E the attractor of the IFS or RIFS in $\mathbf{R}$, the moments of μ are

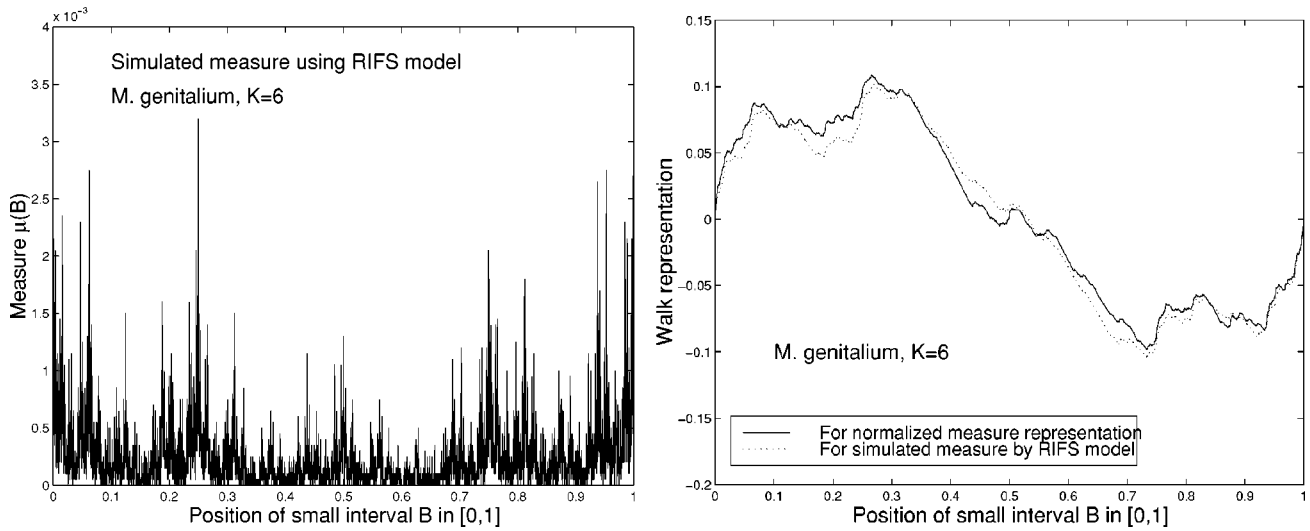$$g_i = \int_E x^i d\mu, \quad g_0 = \int_E d\mu = 1. \tag{15}$$

FIG. 2. Left panel shows simulation of the measure representation (6 strings) of the whole genome of *M. genitalium* using the recurrent IFS model. Right panel shows walk comparison for measure representation (6 strings) of *M. genitalium* and its RIFS simulation.
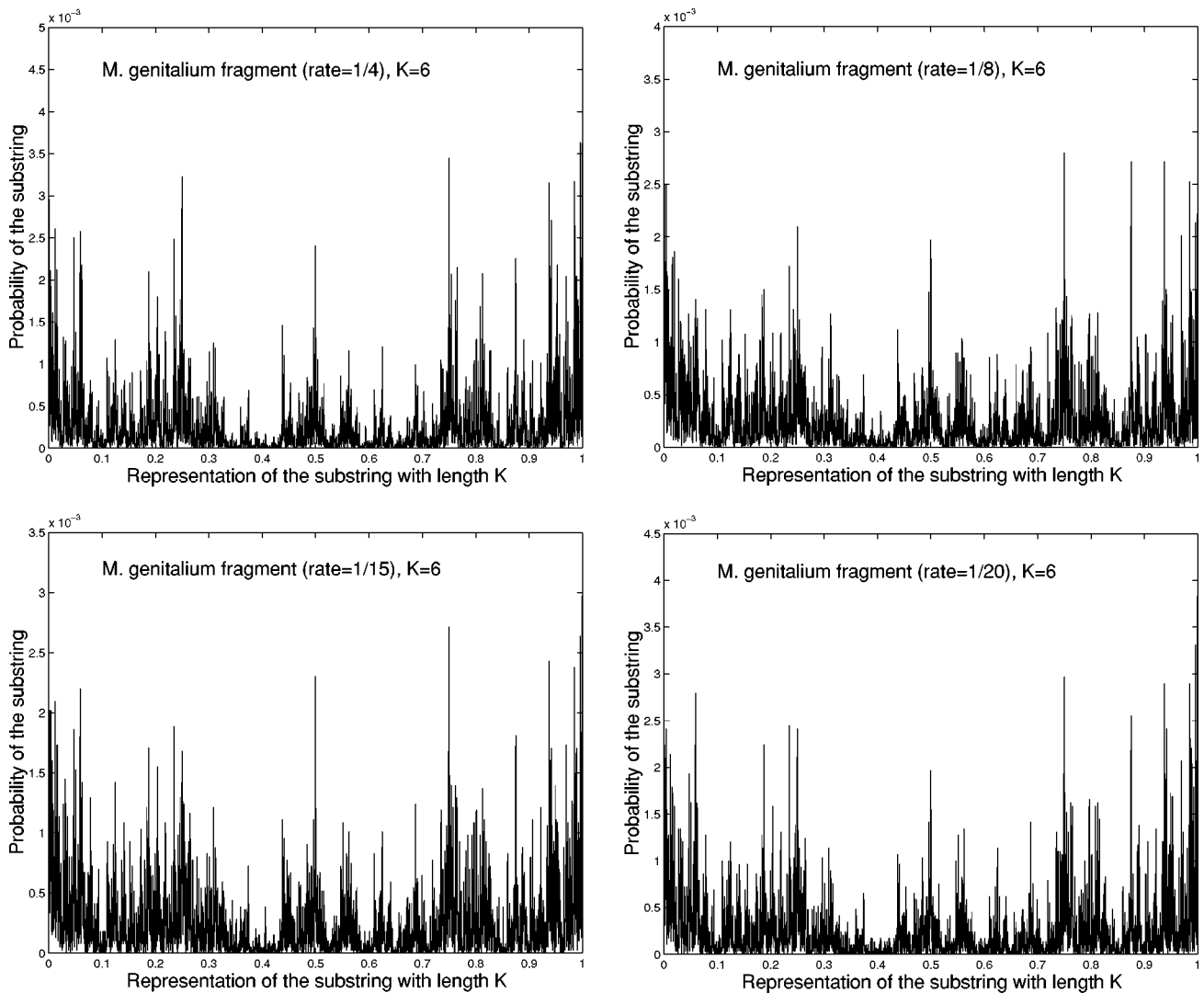

FIG. 3. Histograms of 6 substrings of fragments from *M. genitalium* with different rates.
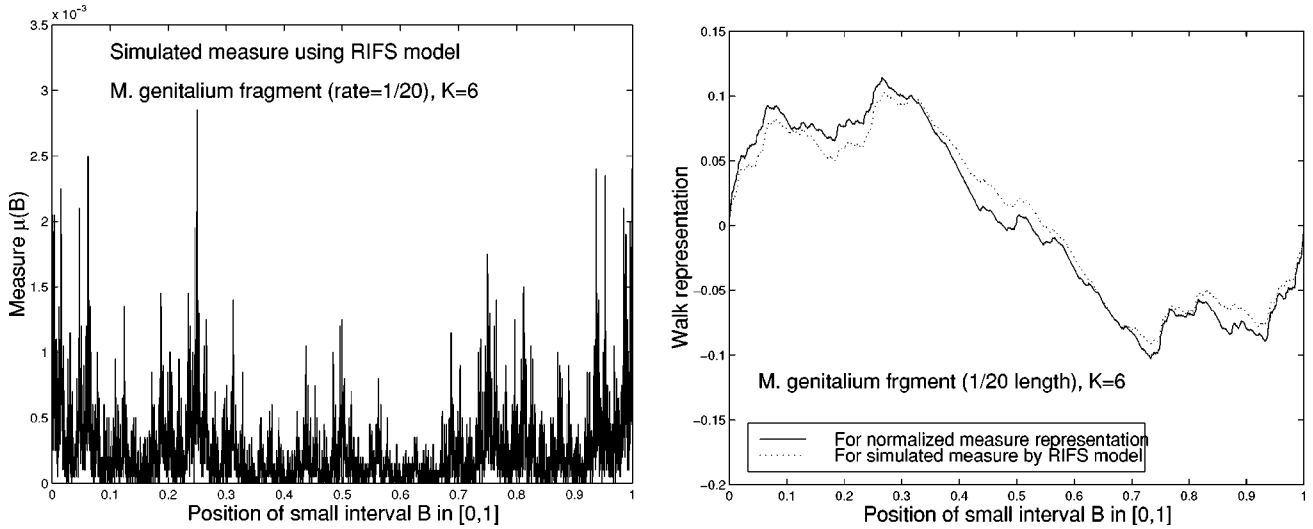
FIG. 4. Left panel shows simulation of the measure representation (6 strings) of 1/20 fragment of *M. genitalium* using the recurrent IFS model. Right panel shows walk comparison for measure representation (6 strings) of 1/20 fragment of *M. genitalium* and its RIFS simulation.

If $S_i(x) = c_i x + d_i$, $i = 1, \ldots, N$, then the following well-known recursion relations hold for the IFS model:

$$\left(1 - \sum_{i=1}^{N} p_i c_i^n\right) g_n = \sum_{j=1}^{n} \binom{n}{j} g_{n-j} \left(\sum_{i=1}^{N} p_i c_i^{n-j} d_i^j\right). \quad (16)$$

Thus, setting $g_0 = 1$, the moments g_n, $n \geq 1$, may be computed recursively from a knowledge of $g_0, \ldots, g_{n-1}$ [38].

For the RIFS model, we have

$$g_n = \sum_{j=1}^{N} g_n^{(j)}, \quad (17)$$

where $g_n^{(j)}$, $j = 1, \ldots, N$, are given by the solution of the following system of linear equations:

$$\sum_{j=1}^{N} (p_{ji} c_i^n - \delta_{ij}) g_n^{(j)} = - \sum_{k=0}^{n-1} \binom{n}{k} \left(\sum_{j=1}^{N} c_i^k d_i^{n-k} p_{ji} g_k^{(j)}\right),$$

$$i = 1, \ldots, N, n \geq 1. \quad (18)$$

For $n = 0$, we set $g_0^{(i)} = m_i$, where m_i are given by the solution of the linear equations

$$\sum_{j=1}^{N} p_{ji} m_j = m_i, \quad i = 1, 2, \ldots, N, \quad g_0 = \sum_{i=1}^{N} m_i = 1. \quad (19)$$

If we denote by G_k the moments obtained directly from a given measure using Eq. (15), and g_k the formal expression of moments obtained from Eq. (16) for the IFS model or from Eqs. (17)–(19) for the RIFS model, then through solving the optimal problem

$$\min_{c_i, d_i, p_i \text{ or } p_{ij}} \sum_{k=1}^{n} (g_k - G_k)^2 \quad \text{for some chosen } n, \quad (20)$$

we can obtain the estimates of the parameters in the IFS or RIFS model.

From the measure representation of a complete genome, it is natural to choose $N = 4$ and

$$S_1(x) = x/4, \quad S_2(x) = x/4 + 1/4,$$

TABLE I. Values of vector representation (P_1, P_2, P_3) of fragments from the five organisms.

| Organism	Sequence	P_1	P_2	P_3
	1/4 Fragment	0.255114	0.248454	0.234208
	1/8 Fragment	0.257610	0.248891	0.232988
A. fulgidus	1/15 Fragment	0.260611	0.245235	0.229882
	1/20 Fragment	0.253536	0.247569	0.233501
	Whole genome	0.257277	0.248579	0.233379
	1/4 Fragment	0.305165	0.160478	0.165485
	1/8 Fragment	0.303635	0.160063	0.166952
B. burgdorferi	1/15 Fragment	0.351298	0.188586	0.135497
	1/20 Fragment	0.310800	0.163463	0.162279
	Whole genome	0.335605	0.173103	0.143191
	1/4 Fragment	0.293139	0.226877	0.197907
	1/8 Fragment	0.275901	0.220717	0.206184
C. trachomatis	1/15 Fragment	0.299231	0.226269	0.194245
	1/20 Fragment	0.293706	0.219299	0.192447
	Whole genome	0.284452	0.223418	0.201998
	1/4 Fragment	0.253291	0.253147	0.237551
	1/8 Fragment	0.250753	0.250494	0.240300
E. coli	1/15 Fragment	0.256441	0.248731	0.232963
	1/20 Fragment	0.252115	0.252027	0.237276
	Whole genome	0.248986	0.255393	0.242893
	1/4 Fragment	0.339263	0.165702	0.140649
	1/8 Fragment	0.335415	0.187653	0.158851
M. genitalium	1/15 Fragment	0.337408	0.173610	0.144801
	1/20 Fragment	0.336145	0.182237	0.149540
	Whole genome	0.335212	0.175269	0.147534
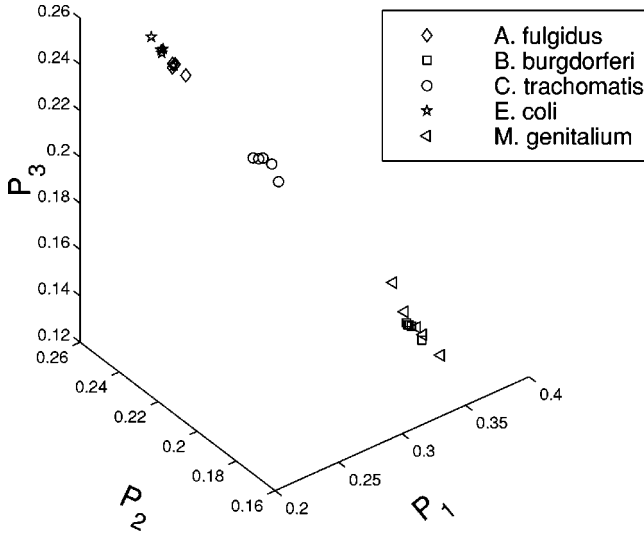
FIG. 5. Vector representation (P_1, P_2, P_3) of all fragments from five organisms.

$$S_3(x) = x/4 + 1/2, \quad S_4(x) = x/4 + 3/4$$

in the IFS or RIFS model. Based on the estimated values of the probabilities, we can use the chaos game to generate a histogram approximation of the invariant measure of the IFS or RIFS, which then can be compared with the given measure of the complete genome.

V. APPLICATION TO THE RECOGNITION PROBLEM

The measure representations for a large number of complete genomes, as described in Sec. II, were obtained in Yu *et al.* [31]. It was found that substrings with $k=6$ seem to provide a limiting measure that can be used for the classification and recognition of DNA sequences. Hence we will use 6 strings in this paper. We then estimated their IFS and RIFS models using the moment method described in Sec. IV. The chaos game algorithm was next performed to generate an orbit as in Eqs. (11) or (12) with Eq. (13). From these orbits, simulated approximations of the invariant measures of IFS or RIFS were obtained via the ergodic theorem (14). In order to clarify how close the simulated measure is to the original measure, we convert a measure to its walk representation: We denote by $\{t_j, j = 1, 2, \ldots, 4^k\}$ the density of a measure and t_{ave} its average, then define the walk $T_j = \sum_{k=1}^{j} (t_k - t_{ave})$, $j = 1, 2, \ldots, 4^k$. The two walks of the given measure and the measure generated by the chaos game of an IFS or RIFS are then plotted in the same figure for comparison. We found that RIFS is a better model to simulate complete genomes. We determine the "goodness" of the measure simulated from the RIFS model relative to the original measure based on the following *relative standard error*, e,

$$e = \frac{e_1}{e_2},$$

where

$$e_1 = \sqrt{\frac{1}{4^6} \sum_{j=1}^{4^6} (t_j - \hat{t}_j)^2},$$

and

$$e_2 = \sqrt{\frac{1}{4^6} \sum_{j=1}^{4^6} (t_j - t_{ave})^2},$$

$(t_j)_{j=1}^{4^6}$ and $(\hat{t}_j)_{j=1}^{4^6}$ being the densities of the original measure and the RIFS simulated measure, respectively. The goodness of fit is indicated by the result $e < 1$. For example, the RIFS simulation of 6-strings measure representation of *M. genitalium* is shown in the left panel of Fig. 2, and the walk of its original 6-strings measure representation and that simulated from the corresponding RIFS are shown in the right panel of Fig. 2. For the whole genome, $e_1 = 0.000\,206\,75$, $e_2 = 0.000\,320\,7$, and $e = 0.6447 < 1$. It is seen that the RIFS simulation fits the original measure very well.

We next pick out five organisms (without any particular *a priori* reason) from about 50 organisms whose complete genomes are currently available. These are *A. fulgidus, B. burgdorferi, C. trachomatis, E. coli*, and *M. genitalium*. Fragments of different length rates ranging from 1/20 to 1/4 and with random starting points along the sequences were then selected. Here the length rate of a fragment means the length of this fragment divided by the length of the genome of the same organism. For example, the measure representations of different fragments of *M. genitalium* are shown in Fig. 3. The RIFS model for each of these fragments was next estimated. We also show the RIFS simulation of the 6-strings measure representation of the 1/20 fragment of *M. genitalium* in the left panel of Fig. 4. The walk of its original 6-strings measure representation and that of RIFS simulation are shown in the right panel of Fig. 4. For this fragment, $e_1 = 0.000\,231\,69$, $e_2 = 0.000\,354\,75$, and $e = 0.6531 < 1$. Again, the RIFS simulation fits the original measure of this fragment very well.

It should be noted that column i in the matrix **P** describes the activity of similarity S_i in each RIFS. To be able to represent each fragment on a three-dimensional plot, we define

$$P_1 = (p_{11} + p_{21} + p_{31} + p_{41})/4,$$

$$P_2 = (p_{12} + p_{22} + p_{32} + p_{42})/4,$$

$$P_3 = (p_{13} + p_{23} + p_{33} + p_{43})/4. \tag{21}$$

Each fragment is then represented by the vector (P_1, P_2, P_3). The values of these vectors are provided in Table I, and the vectors are plotted in Fig. 5. It is seen that the vectors of the fragments from the same organism cluster together, and this clustering holds for all selected lengths. This accuracy is uniform for all five organisms randomly selected.

In matching a fragment to organism, the D_q curve, which depicts the generalized dimension of the invariant measure as described in Sec. III, can also be used. We computed these
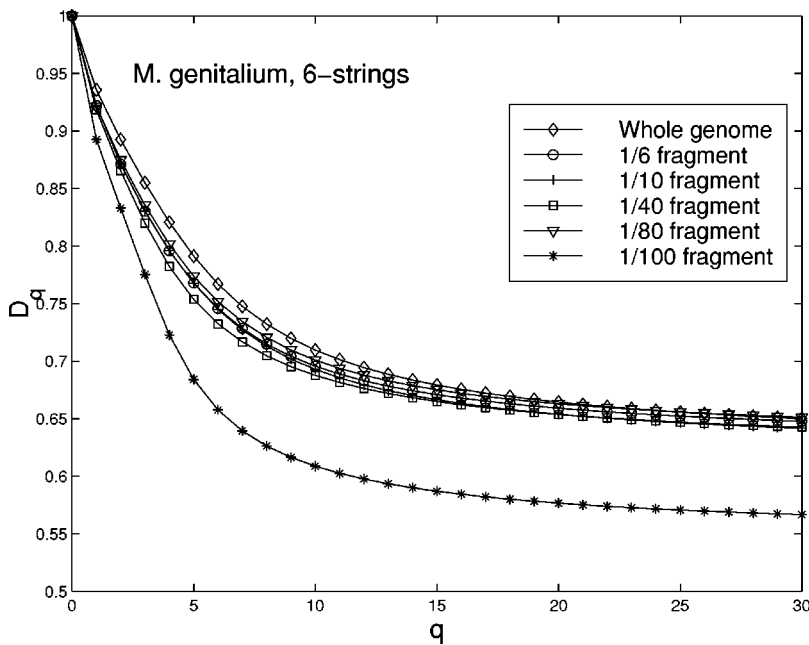
FIG. 6. The dimension spectra of fragments from *M. genitalium*.

curves for the above five organisms at a variety of length sizes, to 1/100th of the original sequence. The results were reported for *M. genitalium* in Fig. 6. It is seen that this method also performs very well. However, it suffers a drawback that many different organisms seem to have the same or closely related D_q curve. In this sense, the method based on the RIFS has higher resolution in distinguishing the genomes. If necessary, the entire matrix **P** may be used, instead of Eq. (21), in this comparison. This would enhance the matching, but will not be as economical as Eq. (21). Yu *et al.* [39] used the entire matrix **P** to define the distance between two organisms in higher-dimensional space and then the evolutionary tree of more than 50 organisms was constructed. The RIFS model can also be used to simulate the measure representation of proteins based on the HP model [40].

VI. CONCLUSION

This paper provides a method for matching fragment to organism taking advantage of the multifractal characteristic of the measure representation of their genomes. It was demonstrated empirically that the underlying mechanism of this multifractality can be captured by a recurrent IFS, whose theory is well founded in the fractal geometry literature. Fast algorithms for the computation of these RIFS and related quantities as well as tools for comparison are available. The method seems to work reasonably well with low computing cost. This fast and economical method can be performed at a preliminary stage to cluster fragments before a more extensive method, such as the random shotgun sequencing method as mentioned in the Introduction, is decided to be brought in for higher accuracy.

[1] W. Li and K. Kaneko, Europhys. Lett. **17**, 655 (1992); W. Li, T. Marr, and K. Kaneko, Physica D **75**, 392 (1994).

[2] C.K. Peng, S. Buldyrev, A.L. Goldberg, S. Havlin, F. Sciortino, M. Simons, and H.E. Stanley, Nature (London) **356**, 168 (1992).

[3] J. Maddox, Nature (London) **358**, 103 (1992).

[4] S. Nee, Nature (London) **357**, 450 (1992).

[5] C.A. Chatzidimitriou-Dreismann and D. Larhammar, Nature (London) **361**, 212 (1993).

[6] V.V. Prabhu and J.M. Claverie, Nature (London) **359**, 782 (1992).

[7] S. Karlin and V. Brendel, Science **259**, 677 (1993).

[8] R. Voss, Phys. Rev. Lett. **68**, 3805 (1992); Fractals **2**, 1 (1994).

[9] H.E. Stanley, S.V. Buldyrev, A.L. Goldberg, Z.D. Goldberg, S. Havlin, R.N. Mantegna, S.M. Ossadnik, C.K. Peng, and M. Simons, Physica A **205**, 214 (1994).

[10] H. Herzel, W. Ebeling, and A.O. Schmitt, Phys. Rev. E **50**, 5061 (1994).

[11] P. Allegrini, M. Barbi, P. Grigolini, and B.J. West, Phys. Rev. E **52**, 5281 (1995).

[12] S.V. Buldyrev, A.L. Goldberger, S. Havlin, R.N. Mantegna, M.E. Matsa, C.K. Peng, M. Simons, and H.E. Stanley, Phys. Rev. E **51**, 5084 (1995).

[13] A. Arneodo, E. Bacry, P.V. Graves, and J.F. Muzy, Phys. Rev. Lett. **74**, 3293 (1995).

[14] A.K. Mohanty and A.V.S.S. Narayana Rao, Phys. Rev. Lett.

84, 1832 (2000).

[15] L. Luo, W. Lee, L. Jia, F. Ji, and L. Tsai, Phys. Rev. E **58**, 861 (1998).

[16] Z.G. Yu and G.Y. Chen, Commun. Theor. Phys. **33**, 673 (2000).

[17] C.L. Berthelsen, J.A. Glazier, and M.H. Skolnick, Phys. Rev. A **45**, 8902 (1992).

[18] C.M. Fraser *et al.*, Science **270**, 397 (1995).

[19] Maria de Sousa Vieira, Phys. Rev. E **60**, 5932 (1999).

[20] Z.G. Yu and B. Wang, Chaos, Solitons Fractals **12**, 519 (2001).

[21] B. Lewin, *Genes VI* (Oxford University Press, Oxford, 1997).

[22] A. Provata and Y. Almirantis, Fractals **8**, 15 (2000).

[23] Z.G. Yu and V.V. Anh, Chaos, Solitons Fractals **12**, 1827 (2001).

[24] Z.G. Yu, V.V. Anh, and Bin Wang, Phys. Rev. E **63**, 11903 (2001).

[25] Z.G. Yu, V.V. Anh, and K.S. Lau, Physica A **301**, 351 (2001).

[26] B.L. Hao, H.C. Lee, and S.Y. Zhang, Chaos, Solitons Fractals **11**, 825 (2000).

[27] Z.G. Yu, B.L. Hao, H.M. Xie, and G.Y. Chen, Chaos, Solitons Fractals **11**, 2215 (2000).

[28] B.L. Hao, H.M. Xie, Z.G. Yu, and G.Y. Chen, Physica A **288**, 10 (2001).

[29] H.J. Jeffrey, Nucleic Acids Res. **18**, 2163 (1990).

[30] N. Goldman, Nucleic Acids Res. **21**, 2487 (1993).

[31] Z.G. Yu, V.V. Anh, and K.S. Lau, Phys. Rev. E **64**, 031903 (2001).

[32] E. Canessa, J. Phys. A **33**, 3637 (2000).

[33] V.V. Anh, K.S. Lau, and Z.G. Yu, J. Phys. A **34**, 7127 (2001).

[34] M.F. Barnsley, J.H. Elton, and D.P. Hardin, Constr. Approx. B **5**, 3 (1989).

[35] K.S. Lau and S.M. Ngai, Adv. Math. **141**, 45 (1999).

[36] T. Halsy, M. Jensen, L. Kadanoff, I. Procaccia, and B. Schraiman, Phys. Rev. A **33**, 1141 (1986).

[37] M.F. Barnsley and S. Demko, Proc. R. Soc. London, Ser. A **399**, 243 (1985).

[38] E. R. Vrscay, in *Fractal Geometry and Analysis*, Vol. 346 of *NATO Advanced Study Institute*, *Series C: Mathematical and Physics Sciences*, edited by J. Belair (Kluwer Academic, Dordrecht, The Netherlands, 1991).

[39] Z.G. Yu, V.V. Anh, K.S. Lau, and K.H. Chu, (unpublished).

[40] Z.G. Yu, V.V. Anh, and K.S. Lau, (unpublished).